

Comparison of environmental performance of modern copper smelting technologies

Christina Alexander^a, Hannu Johto^{b,*}, Mari Lindgren^a, Lauri Pesonen^b, Antti Roine^a

^a Metso Outotec Finland Oy, Kuparitie 10, FI-28330, Pori, Finland

^b Metso Outotec Finland Oy, Rauhalanpuisto 9, FI-02231, Espoo, Finland

ARTICLE INFO

Keywords:

Life cycle assessment
Copper
Pyrometallurgy
Carbon footprint
Greenhouse gases

ABSTRACT

The fight against climate change has emphasized the importance of understanding the environmental performance of metal production technologies. This is especially true for copper whose consumption will increase significantly due to electrification and, therefore, understanding the associated footprint becomes essential. This study uses simulation-based life cycle assessment (LCA) together with a commercial flowsheet simulation program to compare several copper smelting technologies against each other when producing metallic blister copper from sulfide copper ore. The lowest LCA values for three concentrate compositions and three capacities were obtained for Flash Smelting technology with Peirce-Smith converting (FSF-PSC). The unit CO₂ emissions decreased with increasing capacity. The reduction obtained when the capacity was doubled was 1–9%, depending on the technology. The main source of CO₂ emissions was electricity generation, including the use for oxygen production. For instance, for FSF-PSC it accounted for 91% of the climate change when global data source was used for electricity, translating into an 80% reduction if non-fossil electricity was introduced. A reduction of up to 85% in climate change can be achieved by changing from the highest emission producing technology, the Side Blowing Furnace – Top Blowing Converter (SBF-TBC), to the lowest (FSF-PSC) and by using non-fossil electricity.

1. Introduction

Copper is considered as an enabler to a greener future and, therefore, the environmental impact of its production is of high interest. The world copper mine production was about 20 million tonnes in 2018 and the average growth rate has been 2% (ICSG, 2019). However, the mass adaptation of electric vehicles (EV) will create additional demand for copper (Nguyen et al., 2021).

The majority (80%) of annual primary copper production is extracted by pyrometallurgical processes and the rest with hydrometallurgical technologies, typically in connection with in-situ leaching. The typical process steps in the pyrometallurgical processing are smelting, converting, fire-refining and anode casting followed by tankhouse electro-refining to copper cathode. Slag is further cleaned in a slag cleaning furnace or directed to slag flotation. The SO₂ gas generated during the smelting stage is led to an acid plant to produce sulfuric acid (Schlesinger et al., 2011).

Copper it is not the most energy-intensive metal to produce (Norgate et al., 2007) but the growing global demand (Kuipers et al., 2018) and declining ore grades (Northey et al., 2014) are likely to result in

increasing environmental footprint. Ekman Nilsson et al. (2017) reviewed literature for carbon footprint of copper production. Their data did not show any correlation between the processing technology, geographical location and the carbon footprint. The reason could be that the critical factors determining the overall energy consumption: ore type, mining method and processing technology all varied at the same time. On the other hand, in the time-series analysis on environmental impact of copper production in Australia between 1940 and 2008 (Memary et al., 2012) the effects of those factors could be seen for a single production site, but any mutual comparison of the technologies was not possible.

One approach to overcome the difficulty of getting consistent and comparable data is to use simulation-based environmental footprint assessment (Abadías-Llamas et al., 2019). The methodology consists of flow sheet modelling for each smelting process which enables the calculation of heat and mass balances and energy consumption for each process option. Energy consumption in auxiliary unit operations and energy equivalents for process supplies can be computed from a set of unit energy consumption factors. Coursol et al. (2010) used process models done with Metsim software to compare energy demands of four smelting technologies: Flash Smelting and Flash Converting, Top

* Corresponding author.

E-mail address: hannu.johto@mogroup.com (H. Johto).

Submerged Lance smelting and Peirce-Smith Converting, Mitsubishi continuous smelting process and Noranda/Teniente continuous bath smelting and Peirce-Smith converting. Later the results were supplemented with Bottom Blowing technology which is a relatively new technology that has gained ground in China (Watt and Kapusta 2019). Their calculations on the total energy consumption from concentrate to anode copper ranked the technologies in the following order (from lowest energy consumption):

- 1) Flash-Smelting - Flash Converting-Slag Flotation
- 2) Mitsubishi Smelting Process
- 3) Top Submerged Lance – Peirce-Smith Converting – Rotary Slag Cleaning
- 4) Bottom Blowing Smelting – Peirce Smith Converting – Slag Flotation
- 5) Noranda-Teniente with dry feed – Slag Flotation and
- 6) Noranda Reactor (filter cake) - Peirce-Smith Converting – Slag Flotation.

The Flash Smelting had the lowest energy consumption with 10,784 MJ/t of anode copper and the Noranda Reactor the highest energy consumption with 13,072 MJ/t of anode copper. The difference between the lowest and the highest energy consumption values was 21%.

The recent survey (Watt and Kapusta 2019) on copper smelting technologies revealed that the Noranda/Teniente technologies share decreased noticeably from 20% to 8% between 2003 and 2019. At the same time Bottom Blowing technology gained 9% share. The Chinese Side Blowing technology similar to Vanjukov technology was not included in the survey, but it may gain ground in the future. Regarding the converting technologies 76% of copper was produced by Peirce-Smith Converting.

The previous reviews did not, however, reveal much about the individual environmental impacts of using these technologies and, therefore, an attempt was carried out to learn more about this important topic. To the authors' best knowledge, this is the first time when a comprehensive simulation has been conducted to compare the CO₂ emissions of different smelting and converting technologies. The approach is also able to show the effect varying capacity and feed material quality on the results.

2. Methods

Seven different process technologies were compared by using flow-sheet simulation combined with the thermodynamic evaluation of the different process options connected to life cycle assessment (LCA) evaluation tool. The investigated technologies were:

- Flash Smelting (FSF) – Flash Converting (FCF)
- Flash Smelting (FSF) – Peirce-Smith Converting (PSC)
- Top Submerged Lance Smelting (TSL) – Top Submerged Lance Converting (TSLC)
- Top Submerged Lance Smelting (TSL) - Peirce-Smith Converting (PSC)
- Bottom Blowing Reactor (BBR) – Bottom Blowing Continuous Converting (BCC)
- Side Blowing Furnace (SBF) - Top Blowing Converting (TBC)
- Mitsubishi Smelting Process (MSP)

The different smelting routes have in common the intent to reduce external fuel consumption and environmental impact by utilizing the heat of oxidation of the iron and sulfur in the copper concentrate. The technical procedures how each of the different technologies performs the task varies substantially from one to another. The process simulations covered the process from sulfidic copper ore to blister copper but excluded the impact of downstream processes such as fire refining, electrolytic refining, wet gas cleaning and sulfuric acid production since these are performed relatively similarly in all the technologies compared with minor influence on the outcome. In addition, the effect of impurities

and their behavior was not in scope. The main characteristics of these technologies are summarized in Table 1 and described in more detail the following subchapters.

The tool used was the commercial HSC Chemistry software version 9.8 (Roine 2020). and its flowsheet simulation module (SIM) with distribution (pyro) units. The thermodynamic database of the HSC software contains the necessary information (H, S and Cp values) gathered from available literature to perform calculations of the model.

The HSC SIM modelling is based on the graphical flowsheet created by the user with process unit streams required by the technology in calculation. The flows are in case of pyrometallurgical calculations determined by species such as elements or compounds. In each unit, the mass balance of input and output is created by determining the distributions of different elements to both different streams and species in the given streams. The heat balance in the units is calculated by the software based on the enthalpy changes related to both reactions of different compounds in the unit and the changes of enthalpy between incoming and output streams. The models apply multiple controls for the process, including phase compositions (such as matte grade) and temperature in a stream. As an example, the flowsheet of the FSF-FCF process used in this study is shown in Fig. 1.

HSC SIM includes active support for openLCA software, which is an open-source LCA and sustainability software provided by Greendelta (2019). Together with the HSC SIM and openLCA connection, LCA study was done according to the ISO 14040 and 14044:2006 standards to compare the seven selected process technologies.

The goal of the LCA study was to quantify and compare the environmental footprint of the seven different copper smelting process models. The scope, i.e., functional unit and system boundaries, were selected to accompany this goal. The functional unit of the study is 1 tonne of copper in the produced blister copper. Thus, all raw materials, waste disposal, energy consumption, and other flows are based on the production of 1 tonne of copper in the produced blister copper. The system boundaries utilized in the scope are modified “cradle-to-gate”, beginning from the production of raw materials and energy and ending at the copper smelter. However, the production of copper concentrate is not considered, as it is assumed that taking it account would diminish the other differences between the technologies. To prove this, the effect of copper concentrate on the results was calculated for one case.

The inventory analysis was done both in HSC SIM and openLCA. HSC SIM is responsible for the primary inventory data, that is, the direct inputs and outputs of the process based on the simulation results. In openLCA these direct inputs and outputs are mapped into environmental flows, which contain the detailed inventory information. The relevant data to the processes was collected from ecoinvent 3.5 database (Wernet et al., 2016), which ensures the coherence of the values used in comparison for different technologies. The data was limited to global market, meaning that global averages were used from the ecoinvent database.

Based on the environmental flows mapped, the impact assessment was conducted in openLCA. The results of the impact categories are presented in Chapter 4. These results were calculated in climate change (kg CO₂-equivalent, CO₂-eq), fossil depletion (kg oil-equivalent, Oil-eq), and cumulative energy demand (MJ-equivalent, MJ-eq) impact categories using ReCiPe Midpoint (H) and Cumulative Energy Demand-methods (Acero et al., 2020).

2.1. Route 1: Flash Smelting (FSF) – Flash Converting (FCF)

In the flash (suspension) process, fine particles of dry sulfide concentrate, and flux are injected with oxygen enriched air into the furnace in the form of a turbulent divergent jet. (Bryk et al., 1958). FSF requires dry feed charge, produced in this model with a steam dryer. The concentrate, silica flux, converter slag, and slag concentrate together were dried to 0.2% moisture. The dry feed was fed the Flash Smelting furnace together with oxygen enriched process air, with oxygen enrichment up to 85%. The produced slag, with iron to silica (SiO₂) plus lime

Table 1
Main characteristics of the technologies.

| | FSF-FCF | FSF-PSC | TSL-LSLC | TSL-SPC | BBR-BCC | SBF-TBC | MSP |
|---------------------------|------------------------------------|-----------------------------------|--|--|------------------------------------|------------------------------------|--|
| Feed preparation | Steam Dryer Dryer | Steam Dryer Dryer | None (wet to smelting) | None (wet to smelting) | None (wet to smelting) | None (wet to smelting) | Steam Dryer |
| Smelting | Flash smelting | Flash smelting | TSL furnace | TSL furnace | BB smelting | SB smelting | Matte smelting |
| Smelting slag output | Hot to slag pot cooling | Hot to slag pot cooling | Shared launder to EF slag/matte settling | Shared launder to EF slag/matte settling | Hot to slag pot cooling | Hot to slag pot cooling | Shared launder to EF slag/matte settling |
| Smelting matte output | Granulation | Hot to ladles | | | Launder to BCC | Launder to SFF | |
| Smelting slag cleaning | Slag concentrator | Slag concentrator | Slag concentrator | Slag concentrator | Slag concentrator | Slag concentrator | (none) |
| Matte preparation | Matte mill | (none) | (none) | (none) | Part to pot cooling part as hot | (none) | (none) |
| Converting | Flash converter | PS converting | TSL converter | PS converting | BB converting | TB converting | Matte converting |
| Converting slag output | Granulation and circulation to FSF | Pot cooling and circulation to SC | Pot cooling and circulation to SC | Pot cooling and circulation to SC | Pot cooling and circulation to BBR | Pot cooling and circulation to SFF | Pot cooling and circulation to EF |
| Converting blister output | Hot to launder | Hot to ladles | Hot to launders | Hot to ladles | Hot to launder | Hot to launder | Hot to launder |

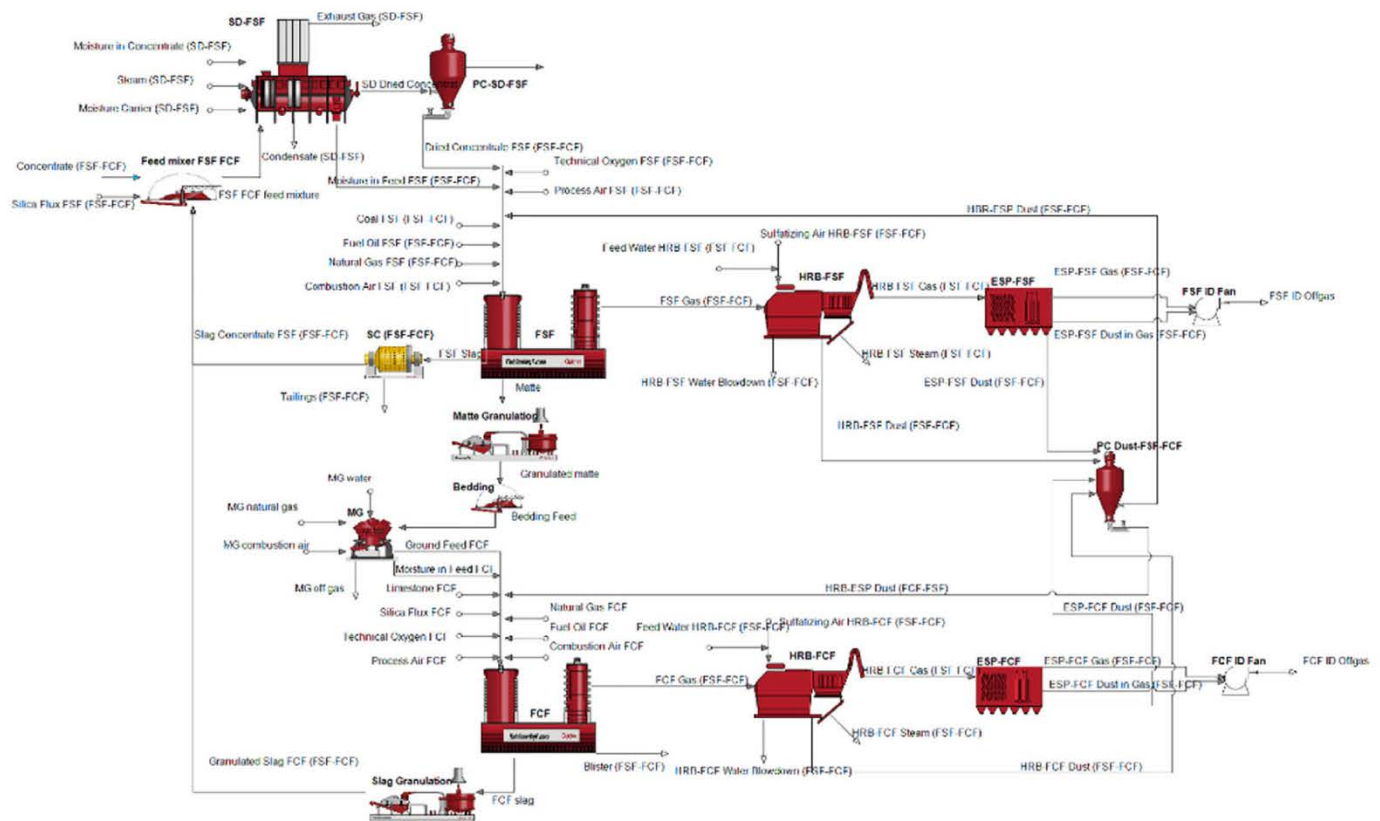


Fig. 1. Flowsheet of the process FSF-FCF from the HSC SIM module with the input and output streams.

(CaO) ratio of 1.35 went for slow cooling and slag flotation. SO₂ rich off-gas of the furnace was cooled in a heat recovery boiler (HRB) and further cleaned from dust in an electrostatic precipitator (ESP) before leading to an ID fan with oxygen content of 0.5% in the off-gas. The elemental distribution to dust used for the FSF was 5%, and the collected sulfatized dust was mixed with FCF dust and recycled in ratio of 75% back to the FSF feed with the balance to the FCF feed.

The matte, with relatively high grade of 67.5% Cu was granulated, milled and dried with a matte mill heated with natural gas (initial matte moisture 5%, outlet 0.2%) before feeding to the FCF together with limestone and silica fluxes and oxygen enriched (enrichment up to 85%) process air. Product copper blister contained residue oxygen and sulfur of 0.3% and 0.2%, respectively together with 0.16% Fe. The FCF slag, with 16% CaO, 2% silica and 19.1% Cu, was granulated and with 5% of

moisture was circulated back to the FSF feed dryer. The off-gas line of the FCF was like the off-gas line of the FSF, while the elemental dust distribution was 2% of the feed components (Metso Outotec 2021).

2.2. Route 2: Flash Smelting (FSF) – Peirce-Smith Converting (PSC)

The FSF is typically operated with a lower matte grade when employing PS Converting instead of an FCF. Otherwise, the FSF works in the same way as in the FSF-FCF route. The elemental distribution to dust used for the FSF was 5%, and the collected sulfatized dust was mixed with converting dust and recycled back to the FSF feed.

The matte, with copper grade of 63% Cu, was transported with ladles to converters, which in the simulation were modelled by using two units. The model calculated the required matte treatment capacity and the

required number of converters, resulting to four vessels, including one under relining. In the first stage, the slag blow, process air with limited oxygen enrichment, 24.5% O₂, was used to produce white metal with 0.3% Fe. The slag, with iron to silica ratio of 1.0 and 10.2% Cu, was poured to ladles, slow cooled and sent to a slag concentrator. Small metallurgical coke addition was used during the slag blowing. The off-gas was led via evaporative cooling towers to a shared ESP and ID fan. The white metal was converted to blister copper during the copper blow, where the blister composition was set to 0.6% O₂, 0.1% S and 0.01% Fe. The slag, with iron to silica ratio of 1.0 results in 25.8% of copper, which was returned to the slag blow step of converting. Process air for the copper blow has an oxygen enrichment of 22.2% and the oxygen in off-gas, treated together with the gas from slag blow, was set to be 2.5% (Metso Outotec 2021; Schlesinger et al., 2011).

2.3. Route 3: Top Submerged Lance Smelting (TSL) – Top Submerged Lance Converting (TSLC)

The TSL smelting furnace can be also operated together with TSL converting (Wood et al., 2017; Metso Outotec 2021). Generally, the processing was performed with similar assumptions than TSL with PSC, but the tapping of matte and slag from the primary smelting furnace was done from separate tapholes. Slag with iron to silica ratio 1.35 was transported to slow cooling while matte with 65% Cu was granulated. Smelting slag was treated in a slag concentrator.

The granulated matte with 5% moisture was fed together with the fluxing agents, silica and limestone, to the TSL converting furnace, where top submerged lance was used for converting the matte with high pressure oxygen enriched air similarly as in the primary smelting furnace. Blister, with 0.6% S and 0.3% O₂, was produced together with converting slag with 8% CaO, 24% Cu and Fe to SiO₂ ratio of 1.8. The converter slag was granulated, and the granulate slag was circulated to the primary furnace. Off-gas was led to HRB and ESP equipped gas line with an ID fan. Sulfatized dust (elemental distribution 0.5%) was collected and circulated back to the converting furnace.

2.4. Route 4: Top Submerged Lance Smelting (TSL) - Peirce-Smith Converting (PSC)

In the top submerged lance type operation, moist concentrate, together with silica flux, thermal coal, circulated dusts and return slag, is fed from the top of the furnace. Vertical top-blown lance is used to inject oxygen enriched (up to 80% with 150 kPa(g)) air direct into melt. The mixture reacts in the molten bath to form a matte and slag emulsion, which continuously overflows through a single melt outlet into an electric settling furnace for matte/slag separation (Biswas and Davenport, 1994; Schlesinger et al., 2011; Wood et al., 2017; Metso Outotec 2021). The matte grade in the TSL furnace was set to be 63% Cu with slag iron to silica ratio of 1.3. Off-gas was led to HRB and ESP equipped gas line with an ID fan. All the sulfatized dust (elemental distribution to dust 0.5%) was collected and circulated back to the feed.

From the electric slag settling furnace, matte was transported via ladles to the converting process and slag, with 0.8% Cu, was tapped for slow cooling and slag flotation. The converting was performed with PSCs with similar assumptions as in the FSF-PSC route, including the slag from slag blown treatment in slag concentrator.

2.5. Route 5: Bottom Blowing Reactor (BBR) – Bottom Blowing Continuous Converting (BCC)

Bottom Blowing smelting and converting technology (BBR-BCC) uses two rotary furnaces linked to each other by continuously flowing hot matte. Both vessels utilize submerged tuyeres which inject oxygen enriched high pressure air from the bottom of the vessel into the molten layer for copper concentrate and matte oxidation. Pressure for the tuyeres was set to 600 kPa(g). Since the furnaces do not have forced cooling

system, a mantle surface temperature of 200 °C was used to calculate the heat losses.

In the BBR, moist concentrate and flux are spread over the bath from the above whereas in the BCC the matte arrives hot from the end wall. In the used HSC-SIM BBR-BCC model, primary smelting furnace produced high grade copper matte with 74% Cu with oxygen enriched (up to 80%) air. The slag with an iron to silica ratio of 1.7 and 26% magnetite was formed with silica addition, skimmed out and treated at a slag concentrator. Off-gas from the furnace was led to HRB and ESP gas line, from where the recovered sulfatized dust, elemental distribution 3% in the furnace, was recycled back to the feed (Zhixiang et al., 2010, 2013, 2013a, 2013b; Yan, 2013, 2014; Yao and Jiang, 2014; Xiaohong et al., 2013; ShuaiBiao, 2016; Jie, 2016; Chen and Zhao, 2016; Qinqing et al., 2016; Qinqing and Xueyi, 2018; Liao et al., 2016; Bing, 2016; Songsong and Xueyi, 2018; Cui et al., 2016).

In the converting vessel, due to the heat loss restrictions, slightly oxygen enriched air (enrichment 24.2%) was used to convert matte to blister with 0.6%, 0.2% and 0.6% S, Fe and O₂, respectively. Part of the matte was tapped to ladle, cooled down and crushed before feeding it to the BCC to control the heat balance (Xia and Liu 2019). Converter slag with an iron to silica ratio of 1.0 and 26% magnetite was produced with silica flux addition, slag was after cooling and crushing circulated back to the BBR. Converter off-gas was treated through an HRB and ESP, and the sulfatized dust was sent to smelting.

2.6. Route 6: Side Blowing Furnace (SBF) - Top Blowing Converting (TBC)

The Side Blowing Furnace process in this simulation has three furnaces: Side Blowing Furnace (SBF), Slag Formation Furnace (SFF), and finally the Top Blowing Converter (TBC) (Xia 2019; Wei et al., 2019). Like in the Mitsubishi process, the matte flows continuously through the first two furnaces before it gets converted in the last one. Due to the similarity to the Vanyukov process, Vanyukov smelting furnace process data was in addition used for reference (Kozhakhmetov et al., 2010, 2013).

The SBF treats moist feed with silica flux and slag concentrate to produce relatively low-grade matte with 56% Cu (Guojun and Qin 2015). Process air with high oxygen enrichment and moderate pressure (150 kPa(g)) was used through the sidewall tuyeres. The resulting slag, with an iron to silica ratio 1.2 and 15% magnetite, was cooled down after tapping and treated in a slag concentrator. The dust, elemental distribution 2% from the furnace feed, and the off-gases are handled through an HRB and ESP. The low-grade matte went via launder to the SFF, where around 35% oxygen enriched air with 150 kPa(g) pressure was used to produce white metal with 3% Fe. The SFF's slag with an iron to silica ratio of 1.8 and 4.5% Cu was also sent to a slag concentrator.

White metal was converted in the TBC using a lance submerged lance system with 150 kPa(g). Blister copper with 0.01% Fe, 0.2% S and 0.6% O₂ was produced. Oxygen enrichment of 28% was used in the process air. The slag was formed with lime addition to contain 7% CaO, silica addition to have an iron to silica ratio of 2.0, 35% magnetite and 28% Cu and it was circulated after cooling and crushing to the SFF. Gases from both converting steps were treated in single off-gas line through a HRB, ESP, ID fan and all the sulfatized dusts were circulated to the SBF.

2.7. Route 7: Mitsubishi Smelting Process (MSP)

The Mitsubishi smelting process is based on three furnaces (S-furnace, CL-furnace and C-furnace) in a sequence with melt flowing downstream in interconnected launders between them (Nagano and Suzuki, 1976; Suzuki et al., 1982; Shibasaki et al., 1993; Goto et al., 1998; Kanç et al., 2003; Tanaka et al., 2003; Hasegawa and Sato, 2003; Schlesinger et al., 2011). Matte with copper grade of 68% was produced from concentrate dried with steam dryer, granulated converter slag, silica and limestone with submerged lances smelting with using oxygen enriched process air with 300 kPa(g). Off-gas from the S-furnace was led via HRB and ESP to

the ID fan. Elemental distribution to dust was set to be 2% and sulfatized dust was recirculated fully to the feed.

Molten slag with an iron to silica ratio of 1.2 and CaO content of 7% flowed continuously from the S-furnace together with matte to the CL-furnace, where matte and slag were separated by settling while electrical energy from the electrodes was used to compensate the heat losses. Discharge slag with 0.8% of copper was tapped out from the process while settled matte flows via launder to converting.

With a similar submerged lance system as with smelting, the C-furnace produces blister, with 0.36% O₂ and 0.15% S, while converting slag with 15% Cu and 18% CaO and 2% SiO₂ was formed with silica and limestone flux addition. The tapped slag was granulated and part of it was recirculated back to the CL-furnace and the rest to the primary smelting furnace, along with dust from the HRB and ESP. No return anode scrap was used as coolant, instead the heat loss was increased to compensate the difference to real world operations.

3. Calculation parameters

In this work, three different concentrates with various copper grades were used to simulate different concentrate types available in the market. For each concentrate, three different capacity scenarios, namely 0.8, 1.2 and 1.6 million tonnes per annum were calculated to evaluate capacity influence without considering possible mechanical restrictions of the furnace constructions. Capacities represent typical furnace treatment capacities required by the market nowadays.

For simplicity, the number of concentrate components was limited, and impurity elements were excluded. The used concentrate grades together with their analysis are presented in Table 2. The term "Others" in table and calculations was used to describe the proportion of additional impurity elements in the concentrate without effect to the main component concentrations. The behavior of "Others" was set in HSC to be in smelting conditions to mimic elements or compounds without chemical reactions, but with phase transformations together with heat effects. The initial moisture of the concentrate was set to typical 8% in the process feed. Feed mixture drying have been included to the models in case the processing technology requires dry feed as described previously.

The composition of the silica sand and limestone fluxes used in the calculations are also presented in Table 2 and were selected to represent average grades (Schlesinger et al., 2011) with moisture of 2%.

In the calculations, the assumed ambient temperature was 25 °C and the plant was located at the sea level. Plant and process air used in the calculations were based on these assumptions. The oxygen enrichment in the processes was performed by adding technical oxygen to the process air, while the technical oxygen content was selected to be 95% with the balance nitrogen.

Additional energy used in the units was either natural gas, coal or electricity, depending on the technology. The amount of additional energy in the processes varied case by case depending on the overall energy balance and standby time, including oxygen enrichment. Natural gas was the additional fuel for FSF, FCF and Mitsubishi S-furnace. Thermal coal

was used in the TSLs, TSLC, BBR and SBF units. The energy for compensating heat losses during standby mode, 50% of the normal heat loss, was produced by natural gas for all the technologies. The compositions of natural gas and thermal coal used are listed in Table 3 along with the composition of coke used for reduction purposes in PSCs and BCC.

The distribution of copper between matte or white metal and slag in a primary smelting furnace is a critical parameter while comparing different smelting methods. In this study, from a large dataset (Metso Outotec 2021), equations for distribution between slag and matte in function of matte grade (i.e. oxidation degree) in industrial operations was created using averages at each matte grade point. The distributions used are given in Equations (1) and (2) for matte and white metal production.

$$(Cu)_{slag} = 0.27691 * [Cu]_{matte}^2 - 0.23201 * [Cu]_{matte} + 0.0541; [Cu]_{matte} < 0.68 \quad (1)$$

$$(Cu)_{slag} = 0.64022 * [Cu]_{matte} - 0.4109; [Cu]_{matte} \geq 0.68 \quad (2)$$

Related to the slag copper content, based on the industrial experience and data, the distribution of copper to compounds in the slag phase was described as a fraction of copper in copper oxide present after slow cooling of the slag as function of matte grade. This fraction is significant because it affects heavily on the copper recovery during the slag cleaning phase. Basically, the fraction of oxide copper is dependent on the amount of sulfur present, which was kept fixed at 0.9%. The higher the oxidation degree and thus the copper content in slag, the higher the oxidized copper content as a percentage. This is a complex topic with many parameters involved so the approach was to keep it as simple as possible in this study without deviating too much from the reality.

Slag cleaning was performed with a slag concentrator in all the other processes than Mitsubishi. Mitsubishi has its own CL-furnace, in which the separation by settling was performed without any reduction. Mitsubishi process is possible to fit with an additional slag concentrator, however according to the authors' knowledge these types of processes are not in commercial use.

The slag concentrator performance was calculated by the distributions of species. In the concentrators, the flotation recovery of metallic copper together with sulfidic copper and iron to the slag concentrate was estimated to be 95% while for the oxidic copper the recovery was 75%. All the other species entering the slag concentrator was given the recovery of 6%. The BBR-BCC process was an exception, because otherwise the discharge slag copper would have been too high with these parameters. Thus, the recovery was increased to 93% for all the copper compounds and 20% for the others, resulting in slag with 0.6% Cu.

All furnace units were dimensioned to obtain the appropriate

Table 2

The compositions of the concentrates and fluxes.

| Component | Conc. low | Conc. avg | Conc. high | Silica flux | Lime flux |
|--------------------------------|-----------|-----------|------------|-------------|-----------|
| | Cu | Cu | Cu | | |
| Component | Wt.% | Wt.% | Wt.% | Wt.% | Wt.% |
| Cu | 22 | 27 | 29 | 0 | 0 |
| Fe | 29 | 26 | 25 | 0 | 0 |
| S | 33 | 31 | 30 | 0 | 0 |
| SiO ₂ | 8 | 8 | 8 | 90 | 0 |
| CaC | 1 | 1 | 1 | 2 | 0 |
| CaCC ₃ | 0 | 0 | 0 | 0 | 90 |
| MgO | 1 | 1 | 1 | 1 | 0 |
| Al ₂ O ₃ | 3 | 3 | 3 | 5 | 0 |
| Others | 3 | 3 | 3 | 2 | 10 |

Table 3

The compositions of natural gas, thermal coal and metallurgical coke.

| Component | Natural gas | Thermal coal | Metal. coke |
|------------------------------------|-------------|--------------|-------------|
| | Wt.% | Wt.% | Wt.% |
| C | 0.0 | 72.93 | 95.5 |
| N ₂ (g) | 5.3 | 4.7 | 0.47 |
| H ₂ (g) | 0.0 | 0.0 | 0.9 |
| S | 0.0 | 0.47 | 0.21 |
| CH ₄ (g) | 88.5 | 0.0 | 0.0 |
| C ₂ H ₆ (g) | 3.6 | 0.0 | 0.0 |
| C ₃ H ₈ (g) | 1.3 | 0.0 | 0.0 |
| C ₄ H ₁₀ (g) | 0.7 | 0.0 | 0.0 |
| C ₅ H ₁₂ (g) | 0.2 | 0.0 | 0.0 |
| CO ₂ (g) | 0.4 | 0.0 | 0.0 |
| SiO ₂ | 0.0 | 4.9 | 1.52 |
| CaO | 0.0 | 1.07 | 0.0 |
| Al ₂ O ₃ | 0.0 | 2.94 | 1.4 |
| H ₂ O | 0.0 | 13 | 0.0 |

refractory amounts, annual availability hours, heat loss values and electricity consumptions for the given process. Refractory mass was basically a function of residence time versus needed melt and gas volume flow multiplied by brick thickness on each surface. Annual operation times were full campaign years deducted with major and minor shut-downs and standby situations (Metso Outotec 2021). Heat losses were estimated based on surface area and if they were water or air cooled. Electricity consumption calculations relied on the earlier published work from one of the authors (Pesonen 2017). One spreadsheet containing the above-mentioned items per process unit was prepared and then implemented to the HSC SIM models.

Generally, all results were cross-checked against real life references and literature. Where data was reliable, the authors used the information as such. Where there was a conflict, for example when a parameter applied to a process model produced an impossible outcome (like with the BBR slag flotation), a deviation to the reported data point was made with considerable care.

4. Results

The simulations were run successfully for each process route using a 3x3 matrix of different concentrate compositions/treatment capacity scenarios presented earlier. The results highlight efficiently the differences between the technologies when it comes to comparing their environmental impacts.

First, the inventory analysis results were obtained for the different technologies. As an example, one inventory analysis result is presented for FSF-FCF with the 1.2 Mt/a capacity in Table 4. Material means the inventory flow from HSC SIM and the Ecoinvent reference refers to the mapped flow from the database. Reference is not applicable for elementary flows.

After obtaining the inventory analysis results, the impact assessment results were calculated. The first task was to calculate the environmental footprint of producing blister with and without the concentrate production based on the Ecoinvent reference, market for copper concentrate, sulfide ore, GLO. For this purpose, only one case and scenario was used: the FSF-FCF technology with concentrate grade of 27% and capacity of 1.2 Mt/a. The proportion of the smelter from the total LCA-values is presented in Table 5 as both absolute values and cumulative proportions.

Table 4
Inventory results for the technology FSF-FCF for 1.2 Mt/a capacity.

| | Material | Amount | | | Unit | Ecoinvent Reference |
|---------------|--------------------------|--------------|--------------|---------------|-------|--|
| | | Conc. low Cu | Conc. avg Cu | Conc. high Cu | | |
| Input | Copper concentrate | 4.59 | 3.74 | 3.47 | tonne | [System], market for copper concentrate, sulfide ore, GLO, Allocation, cut-off by classification, ecoinvent database version 3.5. |
| | Electricity | 0.80 | 0.67 | 0.63 | MWh | [System], market group for electricity, medium voltage, GLO, Allocation, cut-off by classification, ecoinvent database version 3.5. |
| | Limestone flux | 0.14 | 0.14 | 0.14 | tonne | [System], market for limestone, unprocessed, RoW, Allocation, cut-off by classification, ecoinvent database version 3.5. |
| | Natural gas | 0.0098 | 0.0089 | 0.0086 | tonne | Mireille Faist Emmenegger, ESU-services, market for natural gas, low pressure, RoW, Allocation, cut-off by classification, ecoinvent database version 3.5. |
| | Refractories | 0.00099 | 0.00086 | 0.00083 | tonne | [System], market for refractory, basic, packed, GLO, Allocation, cut-off by classification, ecoinvent database version 3.5. |
| | Silica flux | 0.55 | 0.34 | 0.28 | tonne | [System], market for silica sand, GLO, Allocation, cut-off by classification, ecoinvent database version 3.5. |
| Output | Water | 6.75 | 5.08 | 4.57 | tonne | NA |
| | Carbon dioxide | 0.080 | 0.077 | 0.0076 | tonne | NA |
| | Copper in copper blister | 1 | 1 | 1 | tonne | NA |
| | Clean off-gas | 6.91 | 4.64 | 3.92 | tonne | NA |
| | Heat, waste | 3.58 | 2.92 | 2.73 | MWh | NA |
| | Refractories | 0.00099 | 0.00086 | 0.00083 | tonne | NA |
| | Sulfur dioxide | 0.0088 | 0.0067 | 0.0061 | tonne | NA |
| | Sulfur trioxide | 0.0017 | 0.0013 | 0.0011 | tonne | NA |
| | Tailings | 3.14 | 2.31 | 2.08 | tonne | NA |
| | Water vapor | 0.54 | 0.45 | 0.42 | tonne | NA |
| | Wastewater | 4.56 | 3.73 | 3.50 | tonne | NA |

Table 5

The calculated environmental impacts with inclusion and exclusion of concentrate production in one copper smelting process with one capacity (FSF-FCF, 27% Cu, 1.2Mt/a).

| | With the effect of concentrate | Without the effect of concentrate | Unit |
|---------------------------------|--------------------------------|-----------------------------------|---------------------------------------|
| Cumulative energy demand | 47 670 | 8 210 | MJ-Eq/tCu in blister |
| | | 17 | % of the effect with concentrate |
| Climate change | 3 130 | 590 | kg CO ₂ -Eq/tCu in blister |
| | | 19 | % of the effect with concentrate |
| Fossil depletion | 810 | 150 | kg oil-Eq/tCu in blister |
| | | 19 | % of the effect with concentrate |

As demonstrated by Table 5, the production of concentrate represents more than 80% of the environmental footprint of the copper production. Because the aim of this work was to compare copper smelting technologies and the impact of smelting technology selection to copper production, in other comparisons the impact of concentrate production was classified out.

The environmental impact calculation results of the seven selected copper smelting process technologies without the impact of concentrate production are presented in Figs. 2–6. The total energy demand of the treatment at constant copper grade of 27% Cu in the concentrate as function of treatment capacity is shown in Fig. 2. Fig. 3 shows the climate change as carbon dioxide equivalent per ton of produced copper in blister as function of concentrate treatment capacity with constant copper grade in the concentrate of 27% Cu. The effect of concentrate grade to climate change is shown in Fig. 4.

Fig. 5 shows the fossil fuel depletion of the blister production with constant concentrate treatment capacity of 1.2 Mt annually with each technology evaluated in this comparison.

The climate change of each technology in comparison with constant copper grade of 27% and treatment rate of 1.2 Mt annually have been

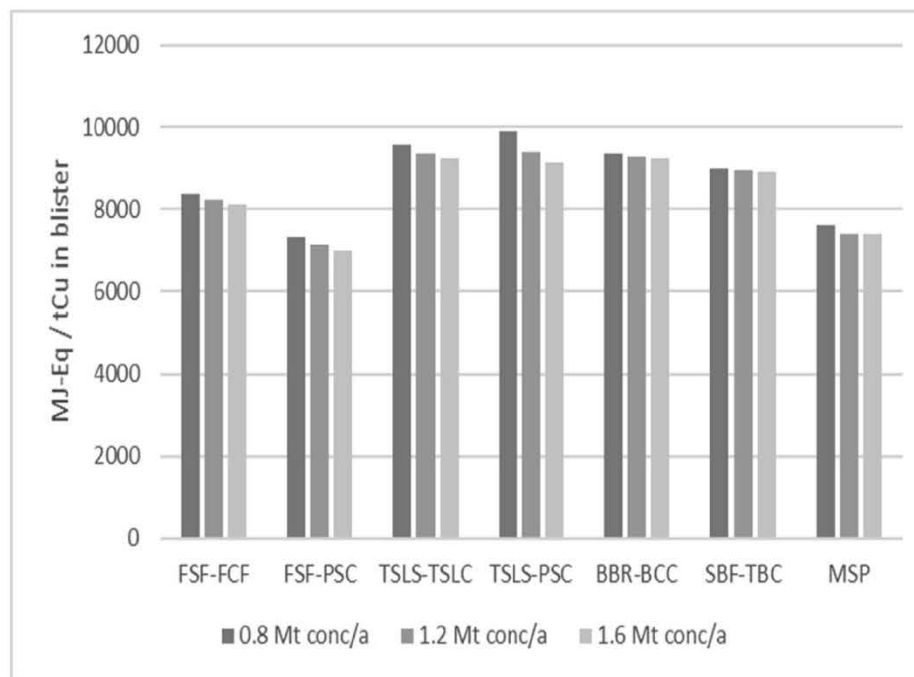


Fig. 2. Calculated total energy consumptions of different technologies with constant copper grade of 27% Cu in concentrate.

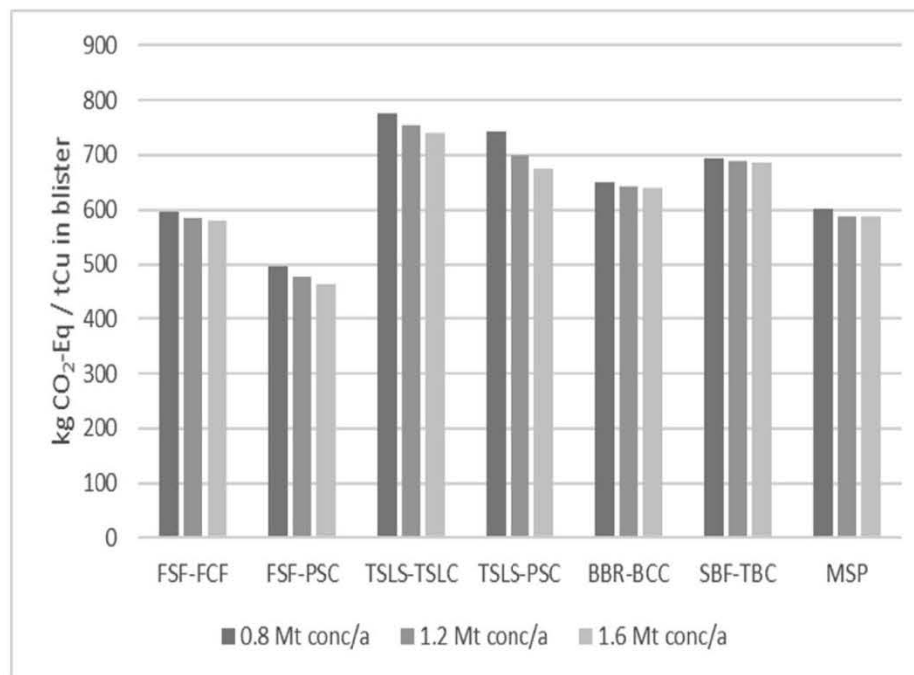


Fig. 3. Calculated climate change of the blister copper production with different production technologies with constant concentrate grade of 27% Cu.

fractionated to emissions related to electricity production and emissions from other sources. Absolute values, together with proportion of the electricity production, are shown in Fig. 6.

These figures shown here represents only a part of the results of this study, which are in more detail shown in Appendix 1. All units are given as per ton of produced copper in blister.

5. Discussion

As outlined by the data in Table 5, the main contribution of

environmental impact of copper production to blister copper comes from the concentrate production at the mine and its transportation to the smelter. This part of the production route represented more than 80% of the impact. This is a slightly higher number than previously given in the literature, 30–70% (Ekman Nilsson et al., 2017; Kulczycka et al., 2017). One contributing factor to the difference is that in the present study the downstream processes, like fire refining or tankhouse electrorefining, were excluded.

The energy consumption values presented in this study were systematically lower than reported for average energy use of copper

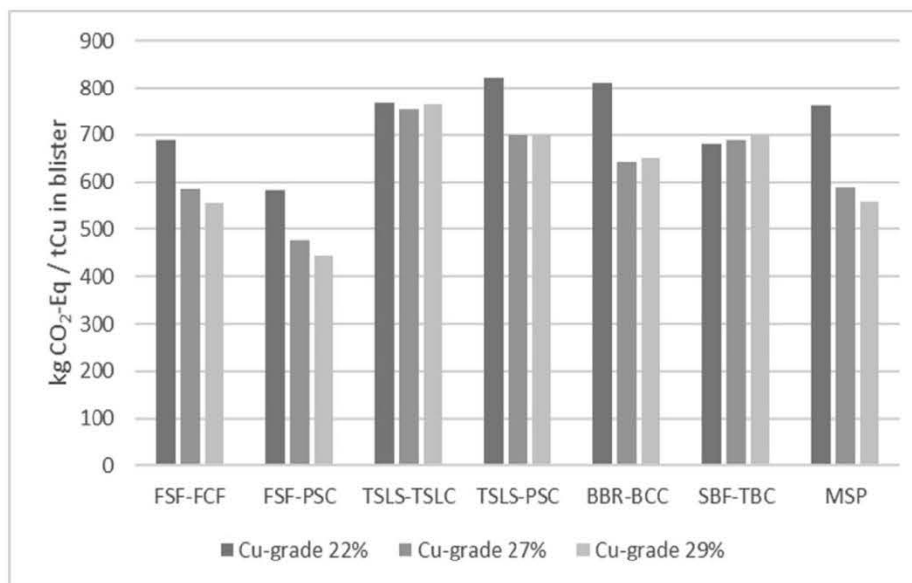


Fig. 4. Calculated climate change of the blister copper production with different production technologies with constant production capacity of 1.2 Mt concentrate annually.

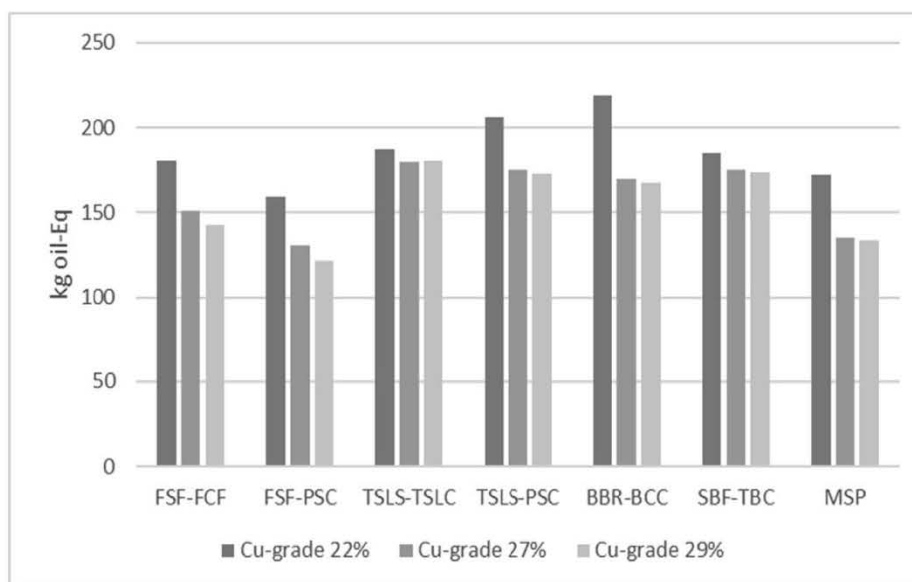


Fig. 5. Calculated fossil fuel depletion of blister copper production with different technologies with constant production capacity of 1.2 Mt concentrate annually.

smelting. BAT documentation (Cusano et al., 2017) provides the energy consumption range of 14–20 GJ/t Cu including the re-smelting of anode scrap and especially the tankhouse electrolysis that is known to consume a significant amount of electricity, about 1.1–1.4 GJ/t Cu. For FSF-FCF we obtained 8.2 GJ Eq/tCu in blister, whereas Coursol et al. (2010) reported 10.8 MJ/t anode for FSF-FCF but their calculations included fire refining, anode casting and the acid plant which automatically lead to a higher energy use. If we include these consumptions, the obtained values in this study are in line with Coursol et al. (2010) but less than in BAT (Cusano et al., 2017).

The reported climate change values are lower compared to 3.3 kg CO₂-eq/kg Cu obtained for pyrometallurgical processing of 3% sulfidic ore (Norgate et al., 2007). Similarly, the differences can be explained by the differences in the system boundaries. Although the smelter operations, which is the scope of this work, represents a minor part of the environmental impacts, it is obvious that also the smelter technology

selection has environmental importance.

Based on the ranking of energy consumptions, the three best techniques of this study were FSF-PSC, MSP and FSF-FCF. In the earlier investigation by Coursol et al. (2010), the energy consumption of FSF-FCF was lower than in MSP but the difference was not great. The results of this study regarding to other technologies were approximately the same as the earlier results (Coursol et al. 2010, 2015) showing that the energy consumption of TSL based technologies and BBR technology were higher than that of FSF-FCF.

The lowest LCA values in all nine concentrate composition and treatment capacity scenarios are with the combination of Flash Smelting technology utilizing PS-Converting technology. The good carbon dioxide equivalent emission data of this technology, together with low energy consumption, are based on energy efficient primary smelting technology with relatively low matte grade. In addition to the efficient primary smelting, the PS-Converting has low equipment energy losses and low

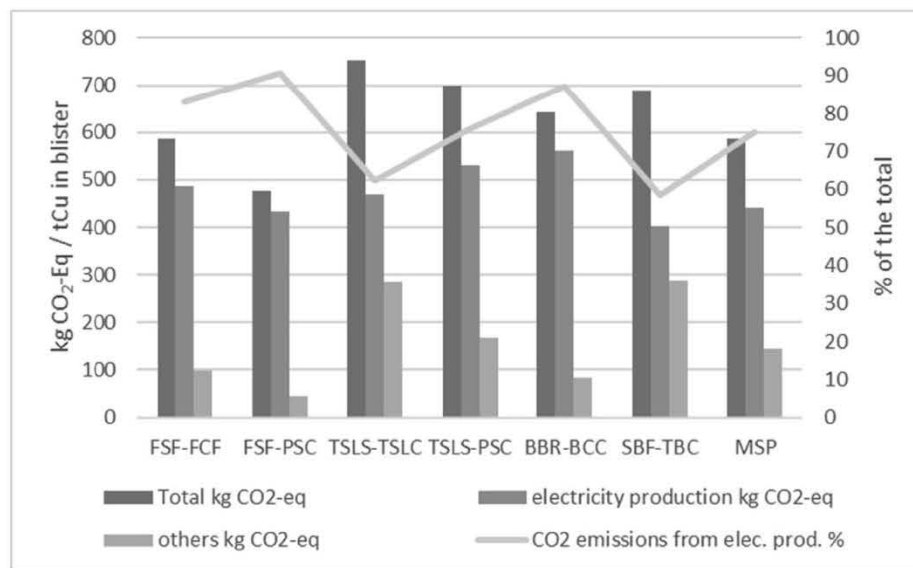


Fig. 6. Proportion of the emissions of the electricity production to the total climate change of each technology in comparison with treatment rate of 1.2 Mt concentrate with 27% Cu annually.

external energy consumption due to low oxygen enrichment of the converting air. Furthermore, the use of only silica flux instead of silica and lime flux mix creates lower environmental footprint, although the slag amount increases to a relatively high value.

On the other hand, a well-established drawback of the PS-Converters is fugitive sulfur emissions compared to the continuous converting technologies (Taskinen et al., 2019). This work does not consider the fugitive emissions, because the level of the emissions is difficult to model and estimate since they are highly dependent on the operational practices and auxiliary equipment design and only weakly dependent on the primary technology solution. It has been earlier stated that the amount of fugitive emissions depends only on the number of units (Coursol et al. 2010, 2015). In addition, the low oxygen enrichment of the blast in the PS-Converters generates high amount of sulfur rich gas to the following sulfuric acid plant (Taskinen et al., 2019). This leads to higher emissions in that section than for the other technologies in this work, but the acid plant emissions were not included in this study.

The Mitsubishi Smelting technology has the advantage of efficient primary smelting and converting with relatively low external energy requirement due to the efficient molten material circulation from one unit operation to another and due to the feeding of dried material to the primary smelting furnace, in this case dried by steam dryer utilizing steam from the process.

The copper recovery in the Mitsubishi CL-furnace in the calculation is relatively low, since no slag reduction is performed with coal or coke addition, meaning that the copper is recovered only by simple melt settling to 0.8% Cu in slag. In addition, the slag amount of Mitsubishi process is high because the ferrous calcium silicate slag is utilized in these furnaces. This is significantly more than with other technologies having a slag concentrator. If reduction would be done, it would create a significant increase in Mitsubishi process carbon dioxide emissions firstly because of the direct increase of carbon addition to the system and secondly by the increased use of electrode electricity in the CL-furnace to compensate the reduction reactions. Alternatively, a slag concentrator could be employed for the same task, but both additions would add to the Mitsubishi process footprint and make it remarkably higher versus what the results show now.

The FSF combined with an FCF has the drawback of requiring solidification and milling of copper matte before the FCF. This may improve the utilization rate of the technology compared to melt movement because the operations are decoupled, but it increases the energy use by

introducing milling and drying operations for the matte, but also because the re-melting solidified matte requires energy through oxygen enrichment of the process gas in the FCF. In addition to the high technical oxygen requirement, FSF-FCF requires, with the calculated raw materials, some additional fuel in the form of natural gas, increasing the environmental impact of the process. Similarly, the use of lime as flux in the converting step instead of silica, increases the carbon footprint of the process, but at the same time decreases the required flux amount.

High coal consumption as an additional fuel combined with the high oxygen enrichment needed increases the environmental footprint of the Side Blow technology, especially with higher copper grade concentrates. The technology utilizes blowing of the process air with elevated pressure to the molten phase which requires extra electricity compared to blower produced air. The fossil depletion of the Side Blow technology, especially with higher copper grades, is among the highest in the comparison due to the high requirement of additional fuel. It appears that the Side-Blow technology requires significant amount of energy, which in case of low concentrate heat value are among the highest calculated in this study. Notable part of this energy is also carbon-based additional fuel.

The TSLS technology together with PS-Converters and TSL Converters, requires, according to this study, high amount of external energy and thus their environmental impacts are high when the copper grade of the feed material is high. With low copper grade the TSL Smelting seems to have relatively good energy efficiency compared to the other studied processes. The PS Converters appears to be more environmentally friendly with higher copper grades of the concentrate while with low copper grades the TSL Converters is more beneficial. The same argumentation for PS Converters as with FSF technology earlier in this paper is valid for combination with TSLS technology.

The Bottom Blowing technology utilizes process air blowing through the bottom to the melt with high pressure resulting in a significant electricity use which has an impact to the environmental performance of the process. The total energy demand of the process is the highest in most of the studied cases. However, the energy source is mostly electricity and the additional fuel consumption is relatively low resulting, especially with cases of higher copper grade in the feed and thus lower slag amount produced, to moderate fossil fuel consumptions and thus moderate climate change.

Regarding the concentrate smelting capacity, it is clear that the higher the treatment capacity the lower the unit process emissions as shown in Figs. 2 and 3. This is because the furnace sizes, and thus heat losses, do

not increase linearly with the processing capacity. This effect, supported by the global trend of increasing smelting unit capacities, would result in lower unit emissions of copper production in the long run. The reduction of emissions with increasing capacity varies between 1% and 9% depending on the technology when the treatment capacity double from 0.8 Mt/a to 1.6 Mt/a. It needs to be pointed out that this work does not take into consideration the technical capacity limitations of different processes, meaning that all seven technologies may not reach the upper capacity in practice. The only proven ones for the highest concentrate treatment capacity, 1.6 Mt annually using one primary smelting unit are with Flash Smelting and TSL Smelting (Watt and Kapusta 2019).

This study evaluated three concentrate copper grades, 22%, 27% and 29% Cu. Different smelting technologies show different trends in their environmental performance when the copper grade varies. As can be seen from Fig. 4, TSLS-TSLC and SBF technologies indicate better environmental performance with decreasing concentrate Cu-grade while other technologies indicate an opposite trend. From the perspective of fossil fuel depletion, Fig. 5, all the technologies have the highest consumption with lowest copper content in the feed, 22% Cu. Thus, the capacity of the plant together with the feed material grade needs to be considered while evaluating the environmental performance of a copper smelter.

The biggest source of emissions with copper smelting comes from the generation of electricity required to operate the plant, including oxygen production, see Fig. 6. It represents, depending on the technology selection, from 58% with SBF-TBC technology to 91% with FSF-PSC technology of the climate change with the global source data of electricity used in this evaluation. Based on this result, it can be estimated, that the climate change of the copper smelting could be reduced by more than 80% by using FSF-PSC, BBR-BCC or FSF-FCF technologies combined with non-fossil electricity source. In opposite, the reduction of climate change by replacing electricity produced with fossil sources with non-fossil electricity is only 58% if SBF-TBC technology is applied.

The climate change of the blister copper produced with different technologies at production capacity 1.2 Mt per annum and 27% Cu in concentrate varies from 753 kg CO₂-eq (TSLS-TSLC) to 477 kg CO₂-eq (FSF-PSC) per t Cu in blister. The decrease of emissions by technology selection represents about 37% of the emissions. In case the electricity in use would be greenhouse gas emission free, the reduction of climate change of copper smelting while changing from the highest emission producing technology (SBF-TBC) to the lowest according to this study (FSF-PSC) would be up to 85%.

Hydrogen burners for metallurgical furnaces are not yet fully industrially proven technology in this field but have potential for further decreasing carbon emissions of the copper production in the future, especially with technologies using currently natural gas or oil as additional fuel such as FSF-PSC, FSF-FCF and MSP, but also possible TSL technologies.

6. Conclusions

Based on the simulation based LCA assessment of different copper

smelting technologies the following conclusions can be drawn:

- The main contributor to the environmental impact is the production and transportation of copper concentrate that accounted for around 80% of the total energy consumption and CO₂ emissions. The smelting technologies studied here in detail only accounted for around 20% of the total impact.
- Of the several technologies investigated, Flash Smelting with Peirce-Smith Converting (FSF-PSC) has the lowest environmental impact for all three concentrate compositions and three capacities.
- The unit CO₂ emissions reduce with increasing capacity for all the technologies. The unit reduction obtained when the capacity doubles is 1–9%, depending on the technology. Top Submerged Lance Smelting - Peirce-Smith Converting (TSLC-PSC) technology is the most sensitive to the capacity change and Side Blowing Furnace - Top Blowing Converting (SBL-TBC) the least.
- For most technologies, CO₂ emissions reduce with increasing copper grade. However, Side Blowing Furnace – Top Blowing Converter (SBF-TBC) technology behaves in an opposite way: its CO₂ emissions increase with the increasing copper grade.
- The main source of CO₂ emissions is electricity use including the one for oxygen production. E.g. for Flash Smelting – Peirce-Smith Converting (FSF-PSC) it accounts for 91% of the climate change when the global data source was used for electricity leading to 80% reduction if non-fossil electricity is introduced.
- In case of non-fossil electricity, the reduction of climate change of copper smelting while changing from the highest emission producing technology Side Blowing Furnace - Top Blowing Converting (SBF-TBC) to the lowest according to this study Flash Smelting – Peirce-Smith Converting (FSF-PSC) would be up to 85%.

CRediT author statement

Christina Alexander: Data curation, investigation. Hannu Johto: Conceptualization, Methodology, Writing- Original draft preparation. Mari Lindgren: Supervision, Writing- Reviewing and Editing. Lauri Pesonen: Conceptualization, Methodology, Editing. Antti Roine: Supervision, Reviewing and Editing.

Declaration of competing interest

The authors declare that they have no known competing financial interests or personal relationships that could have appeared to influence the work reported in this paper.

Acknowledgements

This research was financially supported by the Environmental Handprint Project of Business Finland, Finland.

Appendix A

Table 1

Calculated environmental values of different technologies with copper grade of 22% and capacity of 0.8 Mt/a.

| | TSLS-TSLC | TSLS-PSC | BBR-BCC | FSF-FCF | FSF-PSC | MSP | SBF-TBC | units |
|---------------------|-----------|----------|---------|---------|---------|-------|---------|-----------------------|
| Total energy demand | 10,509 | 11,875 | 12,104 | 9,958 | 9,003 | 9,629 | 10,014 | MJ-Eq |
| Climate change | 797 | 868 | 818 | 700 | 612 | 776 | 687 | g CO ₂ -Eq |
| Fossil depletion | 194 | 217 | 220 | 184 | 165 | 176 | 186 | kg oil-Eq |

Table 2

Calculated environmental values of different technologies with copper grade of 27% and capacity of 0.8 Mt/a.

| | TSLC-TSLC | TSLC-PSC | BBR-BCC | FSF-FCF | FSF-PSC | MSP | SBF-TBC | units |
|----------------------------|-----------|----------|---------|---------|---------|-------|---------|------------------------|
| Total energy demand | 9,580 | 9,889 | 9,358 | 8,357 | 7,308 | 7,593 | 8,985 | MJ-Eq |
| Climate change | 776 | 744 | 651 | 595 | 496 | 601 | 694 | kg CO ₂ -Eq |
| Fossil depletion | 185 | 185 | 172 | 155 | 134 | 140 | 176 | kg oil-Eq |

Table 3

Calculated environmental values of different technologies with copper grade of 29% and capacity of 0.8 Mt/a.

| | TSLC-TSLC | TSLC-PSC | BBR-BCC | FSF-FCF | FSF-PSC | MSP | SBF-TBC | units |
|----------------------------|-----------|----------|---------|---------|---------|-------|---------|------------------------|
| Total energy demand | 9,439 | 9,552 | 9,038 | 7,883 | 6,816 | 7,304 | 8,731 | MJ-Eq |
| Climate change | 787 | 740 | 658 | 564 | 462 | 573 | 703 | kg CO ₂ -Eq |
| Fossil depletion | 185 | 182 | 169 | 146 | 125 | 137 | 175 | kg oil-Eq |

Table 4

Calculated environmental values of different technologies with copper grade of 22% and capacity of 1.2 Mt/a.

| | TSLC-TSLC | TSLC-PSC | BBR-BCC | FSF-FCF | FSF-PSC | MSP | SBF-TBC | units |
|----------------------------|-----------|----------|---------|---------|---------|-------|---------|------------------------|
| Total energy demand | 10,200 | 11,293 | 12,034 | 9,780 | 8,692 | 9,430 | 9,955 | MJ-Eq |
| Climate change | 769 | 821 | 811 | 688 | 582 | 763 | 681 | kg CO ₂ -Eq |
| Fossil depletion | 187 | 206 | 219 | 180 | 159 | 172 | 185 | kg oil-Eq |

Table 5

Calculated environmental values of different technologies with copper grade of 27% and capacity of 1.2 Mt/a.

| | TSLC-TSLC | TSLC-PSC | BBR-BCC | FSF-FCF | FSF-PSC | MSP | SBF-TBC | units |
|----------------------------|-----------|----------|---------|---------|---------|-------|---------|------------------------|
| Total energy demand | 9,351 | 9,395 | 9,283 | 8,211 | 7,130 | 7,380 | 8,935 | MJ-Eq |
| Climate change | 753 | 700 | 643 | 586 | 477 | 587 | 690 | kg CO ₂ -Eq |
| Fossil depletion | 180 | 175 | 170 | 151 | 130 | 135 | 175 | kg oil-Eq |

Table 6

Calculated environmental values of different technologies with copper grade of 29% and capacity of 1.2 Mt/a.

| | TSLC-TSLC | TSLC-PSC | BBR-BCC | FSF-FCF | FSF-PSC | MSP | SBF-TBC | units |
|----------------------------|-----------|----------|---------|---------|---------|-------|---------|------------------------|
| Total energy demand | 9,226 | 9,095 | 8,969 | 7,747 | 6,651 | 7,106 | 8,684 | MJ-Eq |
| Climate change | 766 | 699 | 651 | 555 | 445 | 560 | 699 | kg CO ₂ -Eq |
| Fossil depletion | 181 | 173 | 168 | 143 | 122 | 133 | 174 | kg oil-Eq |

Table 7

Calculated environmental values of different technologies with copper grade of 22% and capacity of 1.6 Mt/a.

| | TSLC-TSLC | TSLC-PSC | BBR-BCC | FSF-FCF | FSF-PSC | MSP | SBF-TBC | units |
|----------------------------|-----------|----------|---------|---------|---------|-------|---------|------------------------|
| Total energy demand | 10,200 | 11,061 | 12,001 | 9,685 | 8,601 | 9,314 | 9,925 | MJ-Eq |
| Climate change | 769 | 802 | 808 | 682 | 572 | 755 | 678 | kg CO ₂ -Eq |
| Fossil depletion | 187 | 202 | 218 | 178 | 157 | 170 | 185 | kg oil-Eq |

Table 8

Calculated environmental values of different technologies with copper grade of 27% and capacity of 1.6 Mt/a.

| | TSLC-TSLC | TSLC-PSC | BBR-BCC | FSF-FCF | FSF-PSC | MSP | SBF-TBC | units |
|----------------------------|-----------|----------|---------|---------|---------|-------|---------|------------------------|
| Total energy demand | 9,234 | 9,117 | 9,247 | 8,133 | 6,982 | 7,380 | 8,909 | MJ-Eq |
| Climate change | 741 | 675 | 640 | 580 | 463 | 587 | 687 | kg CO ₂ -Eq |
| Fossil depletion | 177 | 170 | 170 | 150 | 128 | 135 | 175 | kg oil-Eq |

Table 9

Calculated environmental values of different technologies with copper grade of 29% and capacity of 1.6 Mt/a.

| | TSLC-TSLC | TSLC-PSC | BBR-BCC | FSF-FCF | FSF-PSC | MSP | SBF-TBC | units |
|----------------------------|-----------|----------|---------|---------|---------|-------|---------|------------------------|
| Total energy demand | 9,116 | 8,833 | 9,249 | 7,674 | 6,537 | 6,990 | 8,660 | MJ-Eq |
| Climate change | 755 | 676 | 640 | 550 | 434 | 552 | 696 | kg CO ₂ -Eq |
| Fossil depletion | 178 | 168 | 170 | 141 | 119 | 131 | 173 | kg oil-Eq |

References

- Abadías-Llomas, A., Valero Delgado, A., Valero Capilla, A., Torres Cuadra, C., Hultgren, M., Peltomäki, M., Roine, A., Reuter, M.A., 2019. Simulation-based exergy, thermo-economical and environmental foot print analysis of primary copper production. *Miner. Eng.* 13, 1–65.
- Acero, A.P., Rodríguez, C., Ciroth, A., 2020. LCIA Methods Available online: <https://www.openlca.org/wp-content/uploads/2015/11/LCIA-METHODS-v.1.5.4.pdf>. (Accessed 29 April 2020). <https://doi.org/10.1016/j.jclepro.2020.121822>.
- Bing, L., 2016. Development of Oxygen Bottom-Blowing copper smelting & converting technology. In: *The Proceedings of the Copper 2016 International Conference*. Kobe, Japan, pp. 1265–1272.
- Biswas, A.K., Davenport, W.G., 1994. *Extractive Metallurgy of Copper*, third ed. Elsevier Science Press.
- Bryk, P., Ryselin, J., Honkasalo, J., Malmstrom, R., 1958. Flash smelting copper concentrates. *JOM* 10 (6), 395–400.
- Chen, M., Zhao, B., 2016. Investigation of the accretions in Bottom Blown copper smelting furnace. In: *The Proceedings of the Copper 2016 International Conference*, vols. 1184–1194. Kobe, Japan.
- Coursol, P., Mackey, P.J., Diaz, C.M., 2010. Energy Consumption in Copper Sulphide Smelting. *Proceedings of Copper*, vol. 2. GDMB, Clausthal-Zellerfeld, pp. 649–668. Pyrometallurgy I.
- Coursol, P., Mackey, P.T., Kapusta, J.P.T., Cardona Valencia, N., 2015. Energy Consumption in Copper Smelting: A New Asian Horse in the Race. *JOM*.
- Cui, Zh, Wang, Zh, Wang, H., Wei, Ch, 2016. Two-step copper smelting process at dongying fangyuan. In: *The Proceedings of the Copper 2016 International Conference*, vols. 1043–1052. Kobe, Japan.
- Cusano, G., Rodrigo, M., Farrell, G.F., Remus, R., Roudier, E., Sanchi, L.D., 2017. Best Available Techniques (BAT) Reference Document for the Non-ferrous Metals Industries. Publications Office of the European Union, Luxembourg.
- Ekman Nilsson, A., Macias Aragonés, M., Arroyo Torralvo, F., Dunon, V., Angel, H., Komnitsas, K., Willquist, K., 2017. A review of the carbon footprint of Cu and Zn production from primary and secondary sources. *Minerals* 7, 168–180.
- Goto, M., Oshima, E., Hayashi, M., 1998. Control aspects of the Mitsubishi continuous process. *JOM* 50 (4), 60–63, 65.
- Greendelta, 2019. *OpenLCA 1.8 [Software]*. Software available at: www.openlca.org.
- Guojun, W., Jin, X Jinfeng, 2015. A new player in smelting converting. *Copper Worldwide* 5 (2).
- Hasegawa, N., Sato, H., 2003. Control of magnetite behavior in the Mitsubishi process at Naoshima. In: Kongoli, F., Itagaki, K., Yamauchi, Ch, Sohn, Y.-H. (Eds.), *Proceeding of Yazawa International Symposium Vol. 2, High-Temperature Metal Production*, pp. 509–519 (TMS).
- International Copper Study Group ICSG, 2019. *The World Copper Factbook 2019*. Available online: <http://www.icsg.org/index.php/component/jdownloads/finish/170/2965>. (Accessed 24 April 2020). <https://doi.org/10.1016/j.jclepro.2020.121822>.
- Jie, Y., 2016. Recent operation of the oxygen bottom-blowing copper smelting and continuous copper converting technologies. In: *The Proceedings of the Copper 2016 International Conference*. Kobe, Japan, pp. 1015–1030.
- Kang, C.-Y., Song, H.-L., 2003. Two copper smelting processes at onsan. In: Kongoli, F., Itagaki, K., Yamauchi, Ch, Sohn, Y.-H. (Eds.), *Proceeding of Yazawa International Symposium Vol. 2, High-Temperature Metal Production*. TMS, pp. 317–327.
- Kozhakhmetov, S.M., Kvyatkovskiy, S.A., Ospanov, E.A., Abisheva, Z.S., Zagorodnyaya, A.N., 2010. Processing of high-silicon copper sulfide concentrates by vanyukov smelting. In: *The Proceedings of the Copper 2010 Conference*, vol. 6. Automation and Optimization, Hamburg, Germany, pp. 893–905. Economics Process Control.
- Kozhakhmetov, S., Kvyatkovskiy, S., Abisheva, Z., Bekenov, M., Kamirdinov, G., Semetova, A., 2013. Improvement technology of vanyukov smelting. In: Bassa, R., Parra, R., Luraschi, A., Demetrio, S. (Eds.), *The Proceedings of the Copper 2013 International Conference*, pp. 1059–1063 (Santiago, Chile).
- Kuipers, K.J.J., van Oers, L.F.C.M., Verboon, M., van der Voet, E., 2018. Assessing environmental implications associated with global copper demand and supply scenarios from 2010 to 2050. *Global Environ. Change* 49, 106–115.
- Kulczycka, J., Lelek, L., Lewandowska, A., Wirth, H., Bergesen, J.D., 2017. Environmental impacts of energy-efficient pyrometallurgical copper smelting technologies. *J. Ind. Ecol.* 20, 304–316.
- Liao, L., Qimeng, W., Qinghua, T., Xueyi, G., 2016. Multiphase equilibrium modeling study on the Oxygen Bottom Blowing copper smelting (sks) process. In: *The Proceedings of the Copper 2016 International Conference*. Kobe, Japan, pp. 1252–1264.
- Memary, R., Giurco, D., Mudd, G., 2012. Mason, L. Life cycle assessment: a time-series analysis of copper. *J. Clean. Prod.* 33, 97–108.
- Metso O.totec Oyj (2021) (Technical expert knowledge).
- Nagano, T., Suzuki, T., 1976. Commercial operation of Mitsubishi continuous copper smelting and converting process. In: Yannopoulos, C.J., Agarwal, C.J. (Eds.), *International Symposium on Extractive Metallurgy of Copper Vol. I, Pyrometallurgy and Electrolytic Refining*. The Metallurgical Society and American Institute of Mining, Metallurgical and Petroleum Engineers, pp. 439–458.
- Norgate, T.E., Jahanshahi, S., Rankin, W.J., 2007. Assessing the environmental impact of metal production processes. *J. Clean. Prod.* 15, 838–848.
- Northey, S., Mohr, S., Mudd, G.M., Weng, Z., Giurco, D., 2014. Modelling future copper ore grade decline based on a detailed assessment of copper resources and mining. *Resour. Conserv. Recycl.* 83, 190–201.
- Nguyen, R.T., Eggart, R.G., Severson, M.H., Anderson, C.G., 2021. Global Electrification of Vehicles and Intertwined Material Supply Chains of Cobalt, Copper and Nickel, *Resources, Conservation & Recycling* article (in press).
- Pesonen, L., 2017. Understanding electric energy use at copper smelters. In: *Proceedings of the Conference of Metallurgists 2017*. Canada, Vancouver.
- Qimeng, W., Xueyi, G., 2018. In: Davis, B., et al. (Eds.), *Investigation of the Oxygen Bottom Blown Copper Smelting Process*, The Minerals, Metals & Materials Society, pp. 573–583, 2018, Extraction 2018.
- Qimeng, W., Xueyi, G., Qinghua, T., 2016. Reaction mechanism in an Oxygen Bottom Blown copper smelting furnace. In: *The Proceedings of the Copper 2016 International Conference*. Kobe, Japan, pp. 1239–1251.
- Roine, A., 2020. *HSC Chemistry® [Software]*, Outotec. Software available at: www.outotec.com/HSC.
- Schlesinger, E.M., King, J.M., Sole, C.K., Davenport, I.G.W., 2011. *Extractive Metallurgy of Copper*, fifth ed. Elsevier.
- Shibasaki, T., Hayashi, M., Nishiyama, Y., 1993. Recent operation at Naoshima with a larger Mitsubishi furnace line. In: Landolt, A.C. (Ed.), *Proceedings of the Paul E. Queneau International Symposium on Extractive Metallurgy of Copper, Nickel and Cobalt Vol. II, Copper and Nickel Smelter Operations*, pp. 1413–1428 (TMS and the CIM).
- ShuaiBiao, L., 2016. A review of Oxygen Bottom-Blowing process for copper smelting and converting. In: *The Proceedings of the Copper 2016 International Conference*. Kobe, Japan, pp. 1008–1014.
- Songsong, W., Xueyi, G., 2018. Thermodynamic modeling of oxygen bottom-blowing continuous converting process. In: Davis, B., et al. (Eds.), 445–461, the Minerals, Metals & Materials Society. Extraction 2018.
- Suzuki, T., Yanagida, T., Got, M., Echigoya, T., Kikumoto, N., 1982. Recent operation of Mitsubishi continuous copper smelting and converting process at Naoshima. In: George, B.D., Taylor, C.J. (Eds.), *Proceeding of an International Symposium Copper Smelting – an Update*. TMS of AIME, pp. 51–76.
- Tanaka, F., Iida, O., Takeda, Y., 2003. Thermodynamic fundamentals of calcium ferrite slag and their application to Mitsubishi continuous copper converter. In: Kongoli, F., Itagaki, K., Yamauchi, Ch, Sohn, Y.-H. (Eds.), *Proceeding of Yazawa International Symposium Vol. 2, High-Temperature Metal Production*. TMS, pp. 495–508.
- Taskinen, P., Akdogan, G., Kojo, I., Lahtinen, M., Jokilaakso, A., 2019. Matte converting in copper smelting. *Miner. Process. Extr. Metall. (IMM Trans. Sect. C)* 128, 58–73.
- Watt, L.J., Kapusta, J.P.T., 2019. The 2019 Copper Smelting Survey, *Proceedings of the 58th Annual Conference of Metallurgists (COM) Hosting the 10th International Copper Conference 2019*. Vancouver, Canada, pp. 18–21, 8.2019.
- Wei, W., Tao, L., Weiyang, Y., Bin, T., Wenjiang, L., 2019. Industrial application of Side-Blowing furnace smelting process in China Nerin. In: *Proceedings of the 58th Annual Conference of Metallurgists (COM) Hosting the 10th International Copper Conference 2019*, pp. 18–21, 8.2019, Vancouver, Canada.
- Wernet, G., Bauer, C., Steubing, B., Reinhard, J., Moneno-Ruiz, E., Weidema, B., 2016. The ecoinvent database version 3 (part I): overview and methodology. *Int. J. Life Cycle Assess.* 2, 1218–1230.
- Wood, J., Hoang, J., Hughes, S., 2017. Energy efficiency of the Outotec ausmelt process for primary copper smelting. *JOM* 69 (6), 1013–1020.
- Xia, L., Liu, Zh, 2019. The practice of copper matte converting in China. *Miner. Process. Extr. Metall. (IMM Trans. Sect. C)* 128 (1–2), 117–124.
- Xiaohong, H., Zhifang, L., Kejian, W., Zhenmin, Zh, Liqiong, H., Bing, L., Zhi, W., Fuyong, S., Yue, Y., 2013. Development and application of oxygen bottom-blowing Cu smelting technology. In: Bassa, R., Parra, R., Luraschi, A., Demetrio, S. (Eds.), *The Proceedings of the Copper 2013 International Conference*, pp. 1035–1045 (Santiago, Chile).
- Yan, J., 2013. Latest development of oxygen bottom-blowing copper smelting technology. In: Bassa, R., Parra, R., Luraschi, A., Demetrio, S. (Eds.), *The Proceedings of the Copper 2013 International Conference*, pp. 873–888 (Santiago, Chile).
- Yan, J., 2014. Development of the new oxygen-enriched bottom-blowing continuous copper converting process. In: *The Proceedings of Conference of Metallurgists (COM)* (Published by the Canadian Institute of Mining, Metallurgy and Petroleum).
- Yao, S., Jiang, Ch, 2014. Modern copper smelting and converting technology applications, development, and improvement in China copper industry. In: *The Proceedings of Conference of Metallurgists (COM)*. Institute of Mining, Metallurgy and Petroleum. Published by the Canadian.
- Zhixiang, C., Dianbang, Sh, Zhi, W., Ruimin, B., 2010. A new process of copper smelting with Oxygen enriched bottom blowing technology. In: *The Proceedings of the Copper 2010 Conference*, vol. 6. Automation and Optimization, Hamburg, Germany, pp. 2527–2540. Economics Process Control.
- Zhixiang, C., Zhi, W., Baojun, Zh, 2013. Features of the bottom blown oxygen copper smelting technology. In: Bassa, R., Parra, R., Luraschi, A., Demetrio, S. (Eds.), *The Proceedings of the Copper 2013 International Conference*, pp. 923–934 (Santiago, Chile).
- Zhixiang, C., Zhi, W., Juntao, Zh, Ruimin, L., 2013a. Industrial test development of continuous bottom blown oxygen copper smelting process. In: Bassa, R., Parra, R., Luraschi, A., Demetrio, S. (Eds.), *The Proceedings of the Copper 2013 International Conference*, pp. 1047–1058 (Santiago, Chile).
- Zhixiang, C., Zhi, W., Ruimin, L., 2013b. New development of bottom blown oxygen smelting technology and innovational technologies. In: Bassa, R., Parra, R., Luraschi, A., Demetrio, S. (Eds.), *The Proceedings of the Copper 2013 International Conference*, pp. 935–944 (Santiago, Chile).